Electric Power Systems Research 81 (2011) 2188–2197

Contents lists available at ScienceDirect

Electric Power Systems Research

journal homepage: www.elsevier.com/locate/epsr

Optimal tuning of linear controllers for power electronics/power systems applications

Amin Hasanzadeh[a,*], Chris S. Edrington[b], Hossein Mokhtari[c]

[a] The Center of Advanced Power Systems (CAPS), 2000 Levy Avenue, The Florida State University, Tallahassee, FL 32310, USA
[b] The Florida State University, 600W. College Avenue, Tallahassee, FL 32306, USA
[c] Sharif University of Technology, Azadi Square, Tehran, Iran

ARTICLE INFO

Article history:
Received 30 May 2011
Received in revised form 1 August 2011
Accepted 2 August 2011
Available online 3 September 2011

Keywords:
Linear controllers
Tuning
Optimal control
UPS inverter
Distributed generation

ABSTRACT

This paper presents a new method for tuning various linear controllers such as Proportional–Integral (PI), Proportional–Integral–Derivative (PID) and Proportional–Resonant (PR) structures which are frequently used in power electronics and power system applications. The linear controllers maintain a general structure defined by the Internal Model Principle (IMP) of control theory. The proposed method in this paper is twofold. The first perspective uses the well-known concept of the Linear Quadratic Regulator (LQR) to address the problem as a regulation problem. The Q matrix of the LQR design is then finely adjusted in order to assure the desired transient response for the system. The second perspective redefines the LQR in order to add capability to address the optimal tracking problem and is then generalized to systems with more than two states. These methods are then applied to two specific examples, one in an uninterruptible power supply (UPS) inverter system and the other one in a distributed generation (DG) system. In these examples, the tuning of PR and PI controllers is studied in great detail. These proposed design methods provide an easy and algorithmic procedure without jeopardizing stability or robustness. These tuning methods can also be utilized for linear state-space realization of any power converters. Both examples are supported via simulation and the results, which confirm analytical derivations, are presented and discussed.

1. Introduction

Power electronics and power system applications use various forms of linear controllers such as Proportional–Integral (PI), Proportional–Integral–Derivative (PID) and Proportional–Resonant (PR) controllers, to achieve control objectives mainly specified by the desirable transient and steady-state requirements. Such structures originate from the Internal Model Principle (IMP) of control theory, which states that a model of the desired commands (and disturbances) must exist in the loop to ensure desired steady-state operation and provide that the loop is stable [1]. Thus, a PI (or PID) controller is appropriate for step references and a PR controller for sinusoidal references. The IMP, however, only guarantees the steady-state performance (given that the loop is already stable). The transient response must be controlled by appropriate selection of the controller gains.

There is an abundance of applications for PI, PID and PR controllers in power systems and power electronics systems. Some examples are given below without discussing the details for brevity. In [2], an advanced method is proposed for tuning a PID controller in a hydro-turbine for speed and active power control. PI and PR controllers are used in [3] for parallel and series inverters in a micro-grid power quality compensator. Note that the gains are tuned analytically based on the concepts of phase and gain margins. This concept is developed for a PR controller in [4] for output voltage control of parallel uninterruptible power supplies (UPS). Using a Proportional–Integral-Resonant (PI-RES) for multiple harmonic controls in a Distributed Generation (DG) unit is proposed in [5]. In addition, PR controllers in the stationary reference frame are designed for the series and parallel grid-side converters in a grid connected doubly-fed induction generator (DFIG) wind turbine yielding better dynamic performance during network unbalances [6]. The frequency injection method for tuning of a PID controller in switch mode power supplies is discussed in [7]. PI and PR controllers are also used and analytically tuned for an inverter-based DG unit [8] and also in a multilevel active filter [9]. In [10], a fuzzy-based self-tuning PI is proposed for a thyristor-controlled series capacitor (TCSC) system to improve power system stability. Evolutionary-type algorithms are also used to adjust the fuzzy PID controller gains for an automatic voltage regulator (AVR) [11]. Model predictive control (MPC) is used in [12] to provide on adaptive under-voltage load shedding scheme to protect power systems

* Corresponding author. Tel.: +1 850 570 8771; fax: +1 850 644 7456.
E-mail address: hasanzadeh@caps.fsu.edu (A. Hasanzadeh).

0378-7796/$ – see front matter © 2011 Elsevier B.V. All rights reserved.
doi:10.1016/j.epsr.2011.08.001

against voltage instability. Tuning a PID controller using the LQR method for a multivariable system is presented in [13]. The LQR in [14] adjusts the gains in a multi-loop scheme control of a UPS output voltage. That scheme is however dependent on the output LC-filter parameters and also requires the measurement of the load current. Similar optimal control with LQR can be found in [15] where a real-time emulation is required for loading in a voltage source inverter (VSI). The LQR technique is additionally used in [16] to adjust a multi-loop scheme which is based on a PI controller and the time-derivative of the reference signal in a set of parallel inverters. The work in [17] also uses the LQR technique in combination with dead-beat control to improve the damping of an LCL-filter used to connect a three-phase source to the grid. A nonlinear control of a linearized wind turbine power generation with DFIG is optimized by LQR in [18]. Feedback linearization controls a VSI using pole placement technique to achieve controller coefficients [19].

The well-known and popular concept of LQR offers a highly advantageous method for optimally tuning controller gains in a feedback system; such a method provides appropriate phase-gain margin and variation with respect to nonlinearities [20]. Furthermore, the robustness of a loop can be represented by an interrelation of robust and optimal controllers [21–23]. LQR design can offer high robustness in the subject of system parameter uncertainties, resulting in 60° of phase and infinite gain margins [24]. To apply this method to a regular loop with output feedback, however, the system equations must be put into a state-feedback form. This means that an output feedback controller may or may not be expressible in LQR formulation. The second limitation is that the LQR addresses a regulation problem and cannot originally be applied to a tracking problem, which is desired in practice. These two drawbacks have often been considered as hurdles when working with LQR and have not been systematically addressed in the literature. In this paper, the objective is to overcome these two drawbacks of the LQR method. We are particularly concerned about power system applications, an UPS and a DG system are specific examples addressed in this work.

The proposed technique of this paper is twofold. The first fold finds an optimal Q matrix (in the LQR formulation) which ensures the desired transient response characteristics. This is performed based on the concept of dominant closed-loop poles by mathematically reversing the procedure in the LQR concept formulation. The second approach is based on reformulating and modifying the LQR problem such that optimal tracking is also addressed, i.e. incorporating a "tracking-based" control scheme. The power converters can also employ these tuning methods for their linear state-space realization.

The structure of the paper is as follows. A review of the LQR concept is presented in Section 2. Descriptions of a UPS inverter system and a DG unit as case-study systems are provided in Section 3. Section 4 designs optimal feedback controllers for the case-study systems by optimally tuning the Q matrix based on the concept of dominant poles. An alternative design approach, which directly addresses the tracking problem, is presented in Section 5. It is applied to the UPS and DG unit examples and is generalized to systems with more than two states. Realistic simulation results in PSCAD are presented in Section 6 to verify the analytical results. Section 7 concludes the paper.

2. LQR concept

A linear time-invariant system can generally be described by the following state-space representation

$$\begin{aligned} \dot{x} &= Ax + Bu \quad t > 0 \quad x(0) = x_0 \\ y &= Cx + Du \quad t \geq 0 \end{aligned} \tag{1}$$

where $A \in \Re^{(n\times n)}$, $B \in \Re^{(n\times m)}$, $C \in \Re^{(p\times n)}$, $D \in \Re^{(p\times m)}$ are constant matrices, u is the control signal, x is the state vector, and y is the system output.

The conventional LQR problem is to design a full-state feedback law $u = -Kx$ optimally regulate the states and its output to zero [20]. In the LQR problem, the optimality is measured by

$$J(u) = \int_0^\infty (x^T Q x + u^T R u) dt \tag{2}$$

where $Q = Q^T \in \Re^{(p\times p)}$ is a positive (semi) definite and $R = R^T \in \Re^{(m\times m)}$ is a positive definite matrix. It is shown that the optimal K is given by

$$K = R^{-1} B^T F \tag{3}$$

where the symmetric matrix $F = F^T \in \Re^{(n\times n)}$ is obtained from the Algebraic Riccati Equation (ARE), i.e.

$$A^T F + FA + Q - FBR^{-1}B^T F = 0 \tag{4}$$

The closed-loop dynamics under state feedback law with $u = -Kx$ given by

$$\dot{x} = (A - BK)x = A_{CL}x \tag{5}$$

and the eigenvalues of A_{CL} are the closed-loop poles.

Existence of the solution is under the assumptions that (A,B) is stabilizable, (A,C) detectable, $R > 0$, $Q \geq 0$ and (Q,A) has no unobservable mode on the imaginary axis [20,25]. In addition, R can be chosen unit without lose of generality.

For every given Q matrix, the closed-loop poles are optimally assigned by the LQR solution to achieve optimal regulation. In practice, however, we desire the control system output to track some specific reference command such as a step or a sinusoid. This often requires the addition of another output feedback controller in addition to the state-feedback. Unfortunately, the LQR approach cannot be directly used to optimally design every gain, including those of the state-feedback and of the output feedback. Thus, to overcome this drawback of the method, we propose two methods in this paper. The first method adjusts Q matrix in order to place the closed-loop poles within a specific set in the complex plane which ensures desired tracking (or transient) characteristics. The second method directly addresses the tracking problem.

3. Review of UPS and DG control systems

To develop the proposed optimal tuning method, two specific applications of the method are exemplified. One is a single phase UPS system and the second a *dq* -transformed three phase grid-connected DG system. For both systems, it is shown that the proposed optimal tuning method is successively applied to PR and PI controllers. In this regard, these two systems are described briefly in this section.

3.1. UPS inverter system

Fig. 1 shows the power stage of a single-phase inverter which includes an IGBT half-bridge configuration and an LC-filter. The equivalent series resistance of the filter capacitor is not considered in the model since its effect appears far above the frequency range of concern [26]. The differential equations that describe the large-signal dynamic behavior of this converter are

$$L\frac{di_L}{dt} = \frac{V_{in}}{2}u - v_o - r_L i_L \tag{6}$$

$$i_C = C\frac{dv_o}{dt} = i_L - i_o \tag{7}$$

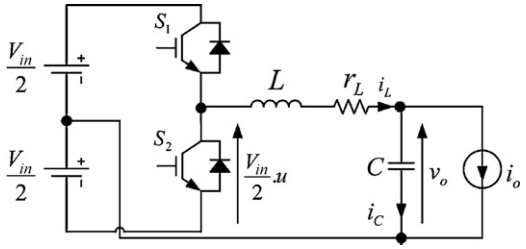

Fig. 1. Power circuit of the single-phase UPS inverter.

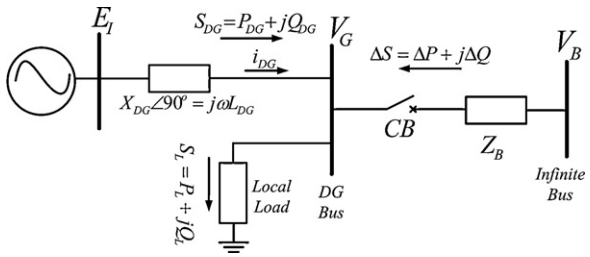

Fig. 3. Single-line diagram of a grid-connected DG system.

where u is the discrete control variable which can take values of 1, 0 or −1 depending on the state of switches S_1 and S_2.

Taking the average from (6) and (7) over one switching period, one can find the state-space equations as:

$$\dot{x}_p = A_p x_p + B_p u + B_w w$$
$$y_p = C_p x_p + D_p u$$

where

$$A_p = \begin{bmatrix} 0 & \frac{1}{C} \\ \frac{-1}{L} & \frac{-r_L}{L} \end{bmatrix} \quad B_p = \begin{bmatrix} 0 \\ \frac{V_{in}}{2L} \end{bmatrix} \quad C_p = \begin{bmatrix} 1 & 0 \end{bmatrix} \quad D_p = 0$$
$$x_p = \begin{bmatrix} v_o \\ i_L \end{bmatrix} \quad y_p = v_o \quad B_w = \begin{bmatrix} \frac{-1}{C} \\ 0 \end{bmatrix} \quad w = i_o \tag{8}$$

The output voltage is thus a function of a continuous control signal u and the output current i_o as given by (9) also shown in Fig. 2

$$V_o(s) = \frac{V_{in}/(2LC)}{s^2 + (r_L/L)s + (1/LC)} U(s) + \frac{(s/C) + (r_L/LC)}{s^2 + (r_L/L)s + (1/LC)} I_o(s) \tag{9}$$

The control objectives in this system are (1) output voltage regulation (resulting in low RMS steady-state error), (2) fast transient response, and (3) low Total Harmonic Distortion (THD). Note that the command waveform and also the disturbance signal are both sinusoids at the fundamental frequency. Based on the IMP, a model of the command/disturbance signal must be incorporated within the controller structure to ensure zero steady-state error. For example, a controller including an integrator can robustly track a step signal, which is the impulse response of an integrator [1]. Therefore, to track a sinusoidal signal, a sinusoidal term must be included in the controller. A so-called PR controller is given

$$G(s) = K_1 + \frac{K_2 s + K_3}{s^2 + \omega_o^2} \tag{10}$$

which is suitable for the system shown in Fig. 2 where ω_o is the system frequency. Design of controller coefficients of K_1, K_2, K_3 to ensure stability and desired optimal performance are the objectives.

3.2. DG system

A DG system works as a power resource through power conditioning AC units such as inverters or AC–AC converters, which can operate either in grid-connected mode or in an islanded mode. The utility grid is modeled by Thevenin Theorem as an equivalent single or three-phase AC source with equivalent internal impedance, Z. Fig. 3 shows a DG unit in grid-connected mode. The output active power, P_{DG}, and reactive power, Q_{DG} from the DG unit to the utility grid should be regulated to reference values P_{ref} and Q_{ref}. A typical control loop of DG system is shown in Fig. 4. The control objectives are including low steady-state error, low current THD, fast response and also low coupling between P_{DG} and Q_{DG}.

Assume that the DG is coupled to the network via an inductance, L_{DG}, and the resistance is neglected. Note, that the presence of this resistance does not increase the model order. Thus, the linear differential equation that describes the large-signal dynamic behavior of this DG unit is

$$L_{DG}\frac{di_{DG}}{dt} = v_I - v_G \tag{11}$$

In a balanced three-phase scenario, the transformation into a synchronous d_q–frame is defined as

$$f_{dq} = f_d + jf_q = \frac{2}{3} e^{-j\theta}\left(f_a + e^{j\frac{2\pi}{3}} f_b + e^{j\frac{4\pi}{3}} f_c\right) \tag{12}$$

where $\theta = \omega_o t + \theta_o$ is the electrical angle of the grid. Then, (11) is transformed into the synchronous reference frame:

$$\frac{di_{DG_{dq}}}{dt} = -j\omega i_{DG_{dq}} + \frac{1}{L_{DG}}(v_{I_{dq}} - v_{G_{dq}}) \tag{13}$$

where $i_{DG_{dq}} = i_{DG_d} + j i_{DG_q}$ is in the synchronous reference frame. Equivalently, (11)–(13) with complex variables can be represented by the following matrix equation:

$$\frac{d}{dt}\begin{bmatrix} i_{DG_d} \\ i_{DG_q} \end{bmatrix} = \begin{bmatrix} 0 & \omega \\ -\omega & 0 \end{bmatrix}\begin{bmatrix} i_{DG_d} \\ i_{DG_q} \end{bmatrix} + \frac{1}{L_{DG}}\begin{bmatrix} v_{I_d} \\ v_{I_q} \end{bmatrix} - \frac{1}{L_{DG}}\begin{bmatrix} v_{G_d} \\ v_{G_q} \end{bmatrix} \tag{14}$$

It is observed that the state-space equations of the d -axis are

$$\dot{x}_d = A_d x_d + B_d u_d + B_{w_1} w_1 + B_{w_2} w_2$$
$$y_d = C_d x_d + D_d u_d$$

where

$$A_d = 0 \quad B_d = \frac{1}{L_{DG}} \quad C_d = 1 \quad D_d = 0 \quad x_d = y_d = i_{DG_d} \quad B_{w_1} = \frac{-1}{L_{DG}} \quad w_1 = v_{G_d} \quad \begin{matrix} B_{w_2} = \omega \\ w_2 = i_{DG_q} \end{matrix} \tag{15}$$

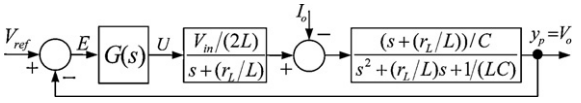

Fig. 2. Block diagram of the UPS inverter control system.

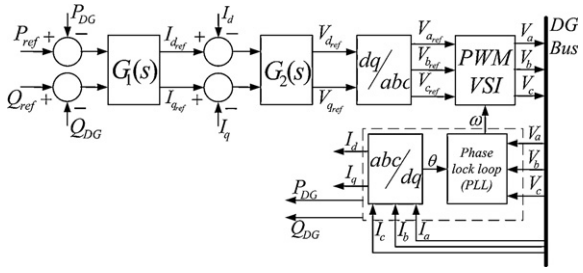

Fig. 4. . A DG unit control block diagram.

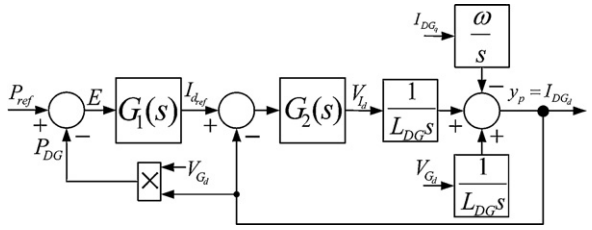

Fig. 5. The *d*-axis of a DG unit system control block diagram.

The output current of the *d*-axis is thus a function of control signal $u_d = v_{I_d}$, DG bus voltage v_{G_d} and the output current of *q*-axis as indicated by (16) and as shown in Fig. 5

$$I_{\mathrm{DG}_d}(s) = \frac{1}{L_{\mathrm{DG}}s}U_d(s) - \frac{1}{L_{\mathrm{DG}}s}V_{G_d}(s) + \frac{\omega}{s}I_{\mathrm{DG}_q}(s) \tag{16}$$

The grid voltage and *q*-axis current can be considered as disturbances or can be compensated using a feed-forward path. The *q*-axis relation is extracted similar to expressions (15) and (16). All signals in *dq*0 -stationary frame have DC characteristics. Thus, according to IMP, integral-type controllers must be used. The PID structure, with the following expression, is a generally accepted type for this application.

$$G_{\mathrm{V-PID}}(s) = K_4 s + \frac{K_5}{s} + K_6 \tag{17}$$

Once again, the objective is to design the controller coefficients of K_4, K_5 and K_5 to achieve stability and desired optimal performance of the DG unit.

4. Tuning of controllers for UPS and DG systems

In this section, tuning of a *PR* controller for a single-phase UPS inverter and a *PI* controller for a three-phase DG grid-connected inverter are optimally designed using state-feedback law and the LQR concept.

4.1. UPS inverter system control

The UPS output voltage control is performed using the output filter inductor current and the output voltage feedbacks. The objectives are to regulate the output voltage to reduce the steady state error, reduce the output voltage THD and improve transient response. Since both state variables are available, we rearrange the UPS control system as shown in Fig. 6. This arrangement has the advantage that it can be transformed into the standard form of an LQR problem. By augmenting the inverter and the *R* controller variables, the following state-space representation is obtained for the closed-loop control.

$$\dot{x} = Ax + Bu \quad u = -Kx$$

where

$$A = \begin{bmatrix} 0 & \frac{1}{C} & 0 & 0 \\ \frac{-1}{L} & \frac{-r_L}{L} & 0 & 0 \\ -1 & 0 & 0 & -\omega_o^2 \\ 0 & 0 & 1 & 0 \end{bmatrix} \quad B = \begin{bmatrix} 0 \\ \frac{V_{in}}{2L} \\ 0 \\ 0 \end{bmatrix} \quad u = -\begin{bmatrix} k_{11} & k_{12} & k_{13} & k_{14} \end{bmatrix} \tag{18}$$

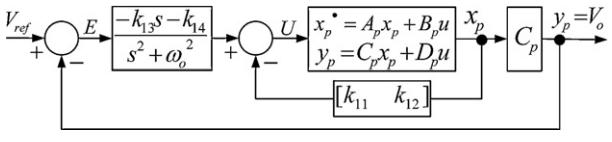

Fig. 6. The UPS inverter system equipped with proposed control structure.

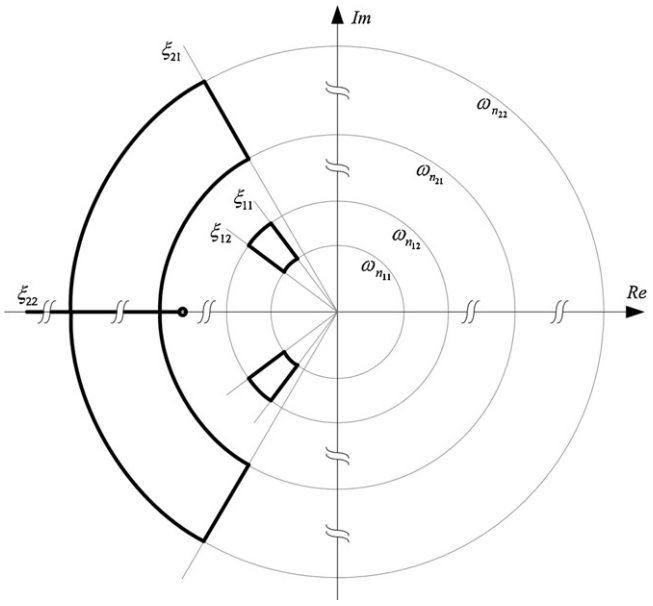

Fig. 7. Desired region for the poles of the UPS control system.

The LQR method can be used to obtain the vector, *K*. The solution, however, depends on *Q* matrix. For every positive semi-definite *Q* matrix, an optimal solution exists. We are particularly interested in a solution which results in a desired tracking response. Such a constraint is not formulated within the LQR structure.

From (18) and by substituting state-feedback law, the closed-loop matrix, A_{CL}, is similar to (5), and thus the closed-loop eigenvalues are obtained from

$$\det(\lambda I - A_{\mathrm{CL}}) = 0 \tag{19}$$

Eq. (19) is a fourth-order polynomial which has four roots. On the other hand, we assume a predetermined region for the closed-loop eigenvalues which correspond to desire tracking features (see Fig. 7).

$$\begin{aligned} &(\lambda^2 + 2\xi_1\omega_{n_1}\lambda + \omega_{n_1}^2)(\lambda^2 + 2\xi_2\omega_{n_2}\lambda + \omega_{n_2}^2) = 0 \\ &0.6 \le \xi_1 \le 0.8 \quad 360 \le \omega_{n_1} \le 600 \quad 0.5 \le \xi_2 \le 2 \quad 1200 \le \omega_{n_2} \le 24000 \end{aligned} \tag{20}$$

This region for parameters is specified based on desired transient response characteristics as a case study. The region includes a subregion for two dominant poles characterized by ξ_1 and ω_{n_1}, which correspond to a desired transient time indicated by a maximum overshoot of 10% and a maximum settling time of one cycle of the line frequency (60 Hz). The second subregion, characterized by ξ_2 and ω_{n_2}, simply indicates a non-dominant region for the rest of the poles. Note that the region for dominant poles is properly selected to avoid very wide bandwidth of the closed-loop system. This improves the noise immunity of the closed-loop system and avoids excessive energy of the control.

Next, the specified region and corresponding Eq. (20) is realized by proper selection of k_{ij} in Eq. (19). Then the reverse procedure in LQR mathematic is started where the k_{ij} determine *F* matrix by using of (3). Next, the *Q* matrix is obtained by (4) where the *Q* matrix must be non-negative though. This means that the problem does not necessarily have a solution or may not have a solution for the entire assigned gain space *K*. In fact, this constraint reduces the predefined and specified region of gain space *K*. In the pie chart of Fig. 8, a simple numerical statistical study by using Table 1 shows that about 63% of the region specified by quadruple $\begin{bmatrix} \xi_1 & \omega_{n_1} & \xi_2 & \omega_{n_2} \end{bmatrix}$ corresponds to a non-negative *Q* and is thus acceptable. There is also another constraint which is imposed by the location of the zero of the *R* controller, i.e. $(-k_3/k_2)$. This zero must not be close to the origin nor must it be

Table 1
Parameters of the UPS inverter power stage.

$L = 0.8$ mH, $V_o = 120\,V_{RMS}$,	$r_L = 0.05\ \Omega$,	$C = 40\ \mu F$, Load (1Φ, $S = 1$ kVA, PF = 0.8)	$V_{in} = 208$ V,	$f_s = 20$ kHz,	$f_o = 60$ Hz,

non-minimum-phase. Enforcing such a constraint will reduce the acceptable range to 46% of the specified region. On the other hand, the statistical result shows that the chance for designers to achieve suitable controller coefficients via a trial and error strategy for controller design is less than 50%, although at the initial stage of this process, the *K*-region in Fig. 7 is designed base on reasonable dominant pole consideration criteria. Now, within the entire acceptable range of *Q*-elements, we search for those which satisfy our additional control specifications such as output voltage regulation and minimal output voltage THD in context of a cost function such as $f(Q) = 100 \times \mathrm{THD}_{v_o} + \left| v_o - V_{o\_\mathrm{Rated}} \right|$ where $Q = diag\{q_1, q_2, q_3, q_4\}$. We arrive at an optimal point using an evolutionary-type algorithm such as Genetic Algorithm (GA) or Particle-Swarm Optimization (PSO). Notice that the search is performed over the acceptable region which is of a reasonable size.

For a single-phase UPS inverter with the power stage parameters given in Table 1, we arrive at the values of the optimally design controller coefficients: $k_{11} = 0.0331$, $k_{12} = 0.0589s$, $k_{13} = -27.397s^{-1}$, $k_{14} = -4903s^{-2}$ from the optimized *Q* matrix. Simulation results of the output voltage versus the reference voltage transient response and the difference (error signal) are shown in Fig. 9(a) and (c), respectively, which proves the desired performance of the proposed IMP based optimal controller including fast tracking around a half cycle of output voltage with no steady-state error. The control signal is also presented in Fig. 9(b) where it illustrates a smooth and reasonable operation, particularly in responding to initiating the output voltage reference at the peak value.

4.2. DG system control

The same procedure that was performed for the UPS system can be applied to the DG unit in *dq*0 -stationary frame. The procedure is only shown for the *d* -axis, but the same strategy can be used for the *q*-axis. The DG unit output control objectives are to reduce the steady-state error, reduce the output current THD, improve transient response and provide low coupling between P_{DG} and Q_{DG} controls. The two control loops for *d* and *q* axes are considered, and for each loop, the current signal is the output which also constitutes the only state variable of the system.

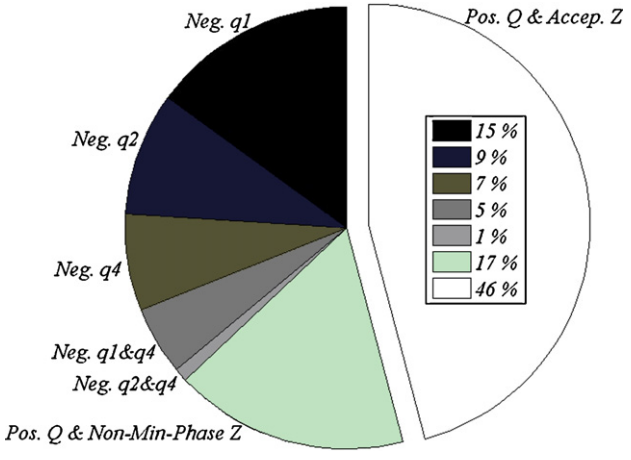

Fig. 8. Resonant controller overall and accepted regions. (Neg. = Negative *Q* elements, Pos. = Positive and accepted *Q* elements, Non-Min-Phase = Non-minimum-phase zero conditions.)

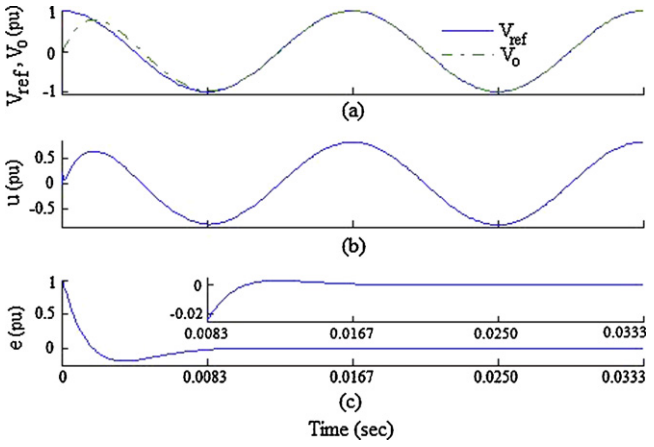

Fig. 9. Performance of the LQR-based controller in the UPS inverter system: (a) output voltage (b) control signal (c) error.

The proposed full-state feedback loop of the system is shown in Fig. 10. This structure is composed of an *I* and a *P* controller. The *P* controller uses the state variable of the system (current signal), and the *I* controller ensures steady-state tracking of the step commands sufficiently. Furthermore, it is not necessary to use a *PI* instead of an *I*, but it is common to do so to improve stability and speed. The controller coefficients are optimally designed in this section. The state-space representation of the system similar to (18) can be shown as

$$A = \begin{bmatrix} 0 & 0 \\ V_{G_d} & 0 \end{bmatrix} \quad B = \begin{bmatrix} \frac{1}{L_{DG}} \\ 0 \end{bmatrix} \quad u = -\begin{bmatrix} k_{21} & k_{22} \end{bmatrix} x \tag{21}$$

Note that V_{G_d} is the grid voltage and can be assumed constant. The desired solution of vector *K* coefficients for this explained LQR problem can be obtained. This solution depends on the positive semi-definite *Q* matrix. Our goal is now to find *Q* such that appropriate transient response is ensured.

Replacing state-feedback law in state-space equation $\dot{x} = Ax + Bu$, the closed-loop matrix A_{CL} is derived as shown in (5). Next, by rearranging the resulting equation in terms of the closed-loop eigenvalues, λ, (22) is obtained:

$$\det(\lambda I - A_{CL}) = \lambda^2 + \left(\frac{k_{21}}{L_{DG}}\right)\lambda + \left(\frac{k_{22}V_{G_d}}{L_{DG}}\right) = 0 \tag{22}$$

Eq. (22) gives a second order polynomial for *P* and *I* controllers coefficients. Now, by following the desired region for the closed-loop, poles can be determined (see Fig. 11)

$$\lambda^2 + 2\xi_3\omega_{n_3}\lambda + \omega_{n_3}^2 = 0 \quad 0.6 \le \xi_3 \le 1 \quad 300 \le \omega_{n_3} \le 500 \tag{23}$$

This region is chosen based on the desired specifications in the transient response as a case study. The design ensures a maximum

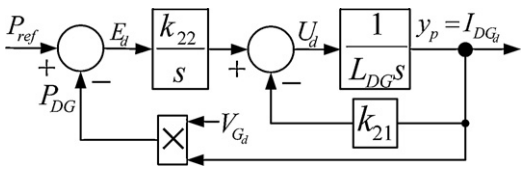

Fig. 10. The DG unit control block diagram with proposed control method.

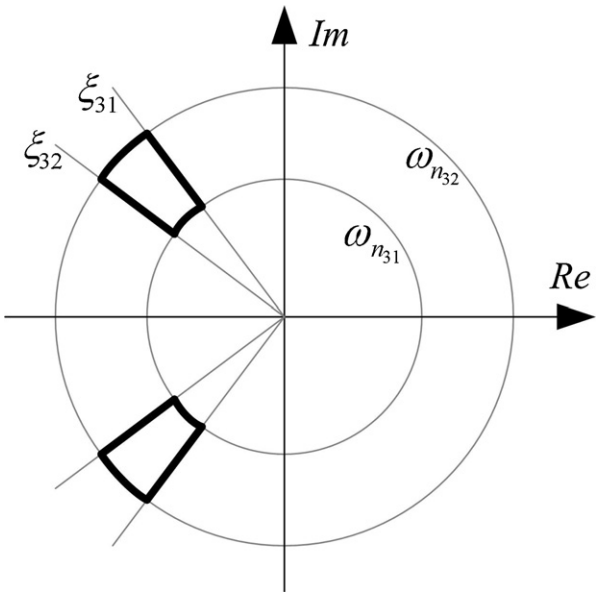

Fig. 11. Desired region for poles of the DG control system.

overshoot of 10% and a maximum settling time of one cycle of the line frequency. Now, comparing (22) with (23), k_{ij} can be found as

$$k_{21} = 2\xi_3\omega_{n_3}L_{\mathrm{DG}} \quad k_{22} = \omega_{n_3}^2 L_{\mathrm{DG}}/V_{G_d} \tag{24}$$

Then, the corresponding elements of the F matrix are obtained by substituting k_{ij} into (3). Finally, the q_{ii} -elements of the Q matrix are achieved by substituting f_{ij} into (4) as:

$$\begin{aligned} q_{11} &= 2(2\xi_3^2 - 1)\omega_{n_3}^2 L_{\mathrm{DG}}^2 \quad & q_{11} \geq 0 \quad \text{if} \quad \xi_3 \geq \sqrt{2}/2 \\ q_{22} &= \omega_{n_3}^4 L_{\mathrm{DG}}^2/V_{G_d}^2 & q_{22} \geq 0 \end{aligned} \tag{25}$$

It can be observed that for the Q matrix to be non-negative the condition $\xi_3 \geq \sqrt{2}/2$ must hold. Thus, the whole set of $[\xi_3\ \omega_{n_3}]$ which satisfy this condition is the acceptable solution. Any selection in this set results in an optimum operation of the system performance.

Next, within the whole acceptable range of Q matrix entries, one can find those which satisfy further control specifications such as the output current THD. This can be done using a fitness function and by means GA. The DG unit parameters are given in Table 2. Applying the proposed procedure to the control parameters results in, $k_{22} = 0.6428 s^{-1}$. The transient response of output active power and the error $k_{21} = 0.5657$ signal are shown in Fig. 12(a) and (c), respectively where they yield the appropriate function of the proposed IMP based optimal controller, including fast tracking around a half cycle of active power delivery with no steady-state error. Furthermore, the control signal is shown in Fig. 12(b) which confirms a satisfactory operation of the controller, including a fast transient to a step change of active power reference command.

5. Alternative design of controllers based on optimal tracking

The previous design strategy, discussed in Section 4, is based on placing the closed-loop poles in a suitable region in the complex plane to ensure desired transient response. In other words, the LQR which can only solve a "regulation" problem is indirectly used to ensure desired "tracking" features. This section shows that the LQR concept can be extended to directly address the optimal tracking problem for those systems. The tracking problem can generally be put in the following framework. Assume that y^* is the command signal and y is the output signal. Moreover, assume that u is the

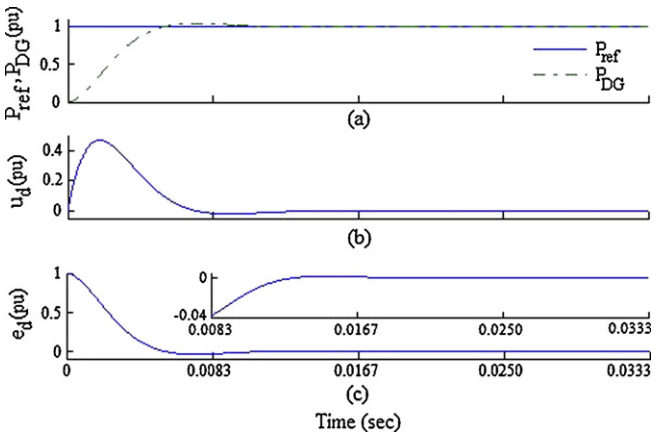

Fig. 12. Performance of the LQR-based controller in a DG system (a) output power (b) control signal (c) error.

control signal and u^* is a desired control signal (at steady-state) which generates y^*. This tracking-based design method can be defined as follows: derive the controller u such that the following index is minimized

$$J(u) = \int_0^\infty (h(y^* - y)^2 + (u^* - u)^2)dt \tag{26}$$

where h is the weight of the tracking term in the fitness function. The challenge is that u^* is not known and even if it is known, it has uncertainties. Now, we address this problem for a UPS and a DG system.

5.1. Rearrangement of the UPS system model

In the case of the UPS inverter system, the command signal y^* is a pure sinusoidal signal at frequency ω_o. This means that all signals will be sinusoids at frequency ω_o at steady-state. Thus, they (including y^*, y and u) all satisfy the equation:

$$\nu = \ddot{u} + \omega_o^2 u = 0 \tag{27}$$

During the transient-time, however, this equation is not heeded. Thus, ν in (27) is an index of how far the signal is from the desired value at time instant, t. Thus, we modify the index function (26) as follows.

$$J(u) = \int_0^\infty (he^2 + \nu^2)dt \tag{28}$$

Now, to formulate a solution to this problem, consider the IMP-based model with sinusoidal input reference as reconfigured in Fig. 13. It is convenient to redefine the state variables in this

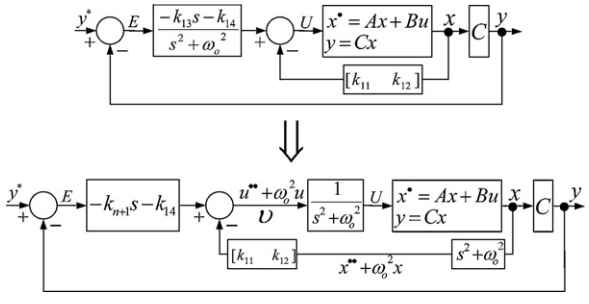

Fig. 13. Reconfiguration of UPS control system for tracking problem.

Table 2
Parameters of the DG power stages.

$L = 0.8$ mH, $V_{oPhase} = 120\,V_{RMS}$,	$r_L = 0.05\,\Omega$,	$V_{in} = 208$ V, S_{ref} (3Φ, $S = 3$ kVA, PF = 0.8)	$f_s = 20$ kHz,	$f_o = 60$ Hz,

system in order to transform the tracking problem into a regulation problem as follows.

$$\dot{\overline{X}} = A\overline{X} + \overline{B}v \quad v = -\overline{K}\overline{X} \tag{29}$$

where

$$\overline{A} = \begin{bmatrix} A & 0 & 0 \\ -C & 0 & -\omega_o^2 \\ 0 & 1 & 0 \end{bmatrix} \quad \overline{B} = \begin{bmatrix} B \\ 0 \\ 0 \end{bmatrix} \quad \overline{X} = \begin{bmatrix} \dot{x} + \omega_o^2 x \\ \dot{e} \\ e \end{bmatrix} \quad \begin{matrix} v = \ddot{u} + \omega_o^2 u \\ \overline{K} = -[\,k_1 \quad \cdots \quad k_n \quad k_{n+1}\ k_{n+2}\,] \end{matrix}$$

Now, the index function can be rewritten as

$$J(u) = \int_0^\infty (he^2 + v^2)dt = \int_0^\infty (\overline{X}^T Q_1 \overline{X} + v^2)dt \tag{30}$$

where

$$Q_1 = \begin{bmatrix} 0 & 0 & 0 & 0 \\ 0 & 0 & 0 & 0 \\ 0 & 0 & 0 & 0 \\ 0 & 0 & 0 & h \end{bmatrix} \tag{31}$$

This means that the tracking problem has been transformed into a regulation problem and the Q_1 matrix in (31) can optimally be addressed.

The proposed technique is applied to the UPS inverter with the power stage specification of Table 1. The control parameters of, $k_{12} = 0.02116s$, $k_{13} = -31.354s^{-1}$ and $k_{14} = -70021s^{-2}$ are obtained for a value of $h = 5 \times 10^9$ which is limited by the signal control −1 to +1 $k_{11} = 0.00436$ limitation especially in first cycle of control signal. The output and reference voltages, their difference as an error signal, and the control signal are shown in Fig. 14. Results of the previous LQR-based design are also shown for comparison. The results of Figs. 14(a) and (c) demonstrate a faster and more accurate output voltage tracking without steady-state error of the output voltage in comparison to the results of the previous LQR-based design. Additionally, Fig. 14(b) shows a fast and stable response of the signal control to the highest value initiation of the output voltage.

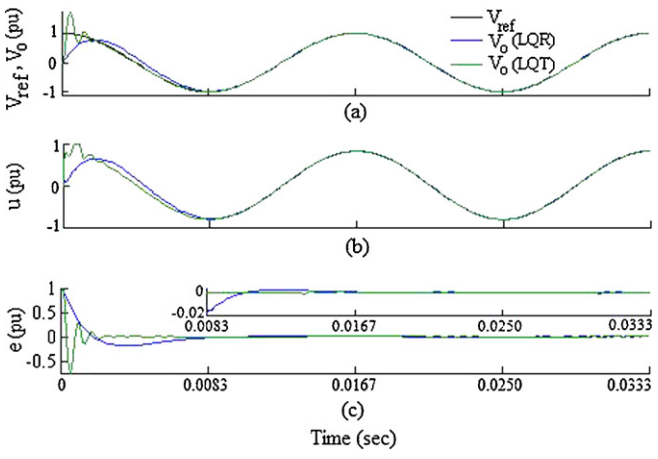

Fig. 14. Performance of the Tracking-based design in the UPS system in compare to LQR-based one (a) output voltage (b) control signal (c) error.

5.2. Rearrangement of the DG unit model

The optimal tracking problem in the DG unit can be expressed as follows. Obtain the controller coefficients such that the following function is minimized

$$J(u) = \int_0^\infty (h(r - Cx)^2 + \dot{u}^2)dt = \int_0^\infty (he^2 + v^2)dt \tag{32}$$

Note that in (32), we have considered the fact that the signals are DC and the derivative is an index for the error. The state-space model of the system is rearranged Fig. 15. With this configuration, the state variables are redefined and the new matrices are

$$\dot{\overline{X}} = \overline{A}\overline{X} + \overline{B}v \quad v = -\overline{K}\overline{X}$$

where

$$\overline{A} = \begin{bmatrix} A & 0 \\ -C & 0 \end{bmatrix} \quad \overline{B} = \begin{bmatrix} B \\ 0 \end{bmatrix} \quad \overline{X} = \begin{bmatrix} \dot{x} \\ e \end{bmatrix} \quad v = \dot{u} \quad \overline{K} = -\begin{bmatrix} k_{21} & k_{22} \end{bmatrix} \tag{33}$$

Now, similar to UPS system with index function of (30), the corresponding Q_1 matrix can be found as

$$Q_1 = \begin{bmatrix} 0 & 0 \\ 0 & h \end{bmatrix} \tag{34}$$

By using this Q_1 matrix, the tracking problem is transformed into a regulation problem which can be solved using LQR method.

The proposed design technique is applied to a DG unit with power stage parameters of Table 2. The resulted control parameters are and $k_{21} = 0.8459$ $k_{22} = -1.4374s^{-1}$ for a value of $h = 2.066$. The suitable fast transient response, without steady-state error of the system, to a step in real power command, and the error signal, are shown in Fig. 16(a) and (c); moreover these results are shown alongside the regulation LQR-based results for easy comparison. Furthermore, the control signal responds rapidly to provide the desired tracking of real output power with respect to the −1 to +1 range restriction, as shown in Fig. 16(b).

5.3. Generalization of the proposed technique

The proposed technique which was tested for the UPS and the DG systems can now be generalized. Assume the feedback controller (based on the IMP) shown in Fig. 17(a). The objective is to design the controller coefficients in order to minimize the cost

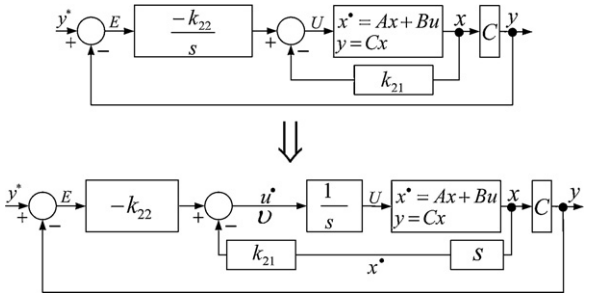

Fig. 15. Rearrangement of DG control system for tracking problem.

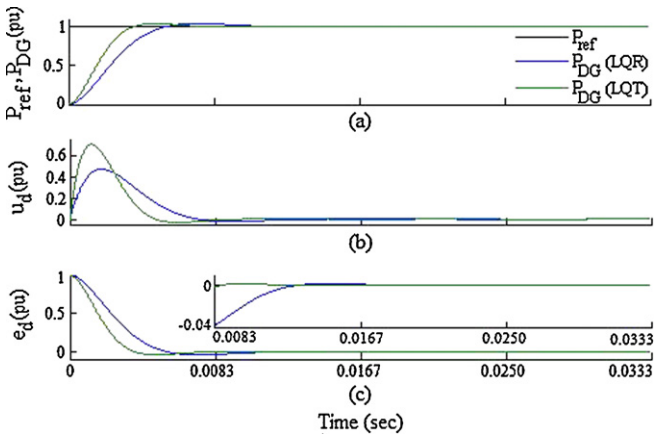

Fig. 16. Performance of the tracking-based design in the DG system in compare to LQR-based one (a) output power (b) control signal (c) error.

function (25). The feedback controller is given by the transfer function $G(s)$ as

$$G(s) = \frac{-k_{n+1}s^{r-1} - k_{n+2}s^{r-2} - \cdots - k_{n+r}}{s^r + g_{r-1}s^{r-1} + \cdots + g_0} = \frac{N(s)}{D(s)} \tag{35}$$

Fig. 17(b) shows a reconfiguration of this system. Define the new control signal as.

$$v = u^{(r)} + g_{r-1}u^{(r-1)} + \cdots + g_0 u = -[k_1 \ \cdots \ k_n \, k_{n+1} \ \cdots k_{n+r}]\,\overline{X} \tag{36}$$

where the new set of state variables $\overline{X}$ is

$$\overline{X}^T_{(n+r)\times 1} = [\, x^{(r)} + g_{r-1}x^{(r-1)} + \cdots + g_0 x \quad e^{(r-1)} \quad e^{(r-2)} \quad \cdots \quad \dot{e} \quad e \,] \tag{37}$$

Thus, we can rewrite the state-space representation of the closed-loop system as

$$\dot{\overline{X}} = \overline{A}_{(n+r)\times(n+r)}\overline{X} + \overline{B}_{(n+r)\times 1}\, v \qquad v = -\overline{K}_{1\times(n+r)}\overline{X}$$

$$\overline{A} = \begin{bmatrix} A & 0 & \cdots & \cdots & \cdots & \cdots & 0 \\ -C & -g_{r-1} & -g_{r-2} & \cdots & \cdots & \cdots & -g_0 \\ 0 & 1 & 0 & \cdots & \cdots & \cdots & 0 \\ \vdots & 0 & 1 & 0 & \cdots & \cdots & 0 \\ \vdots & \vdots & \ddots & \ddots & \ddots & \ddots & \vdots \\ \vdots & \cdots & \cdots & 0 & 1 & 0 & \vdots \\ 0 & 0 & \cdots & 0 & 0 & 1 & 0 \end{bmatrix} \quad \overline{B} = \begin{bmatrix} B \\ 0 \\ \vdots \\ 0 \end{bmatrix} \tag{38}$$

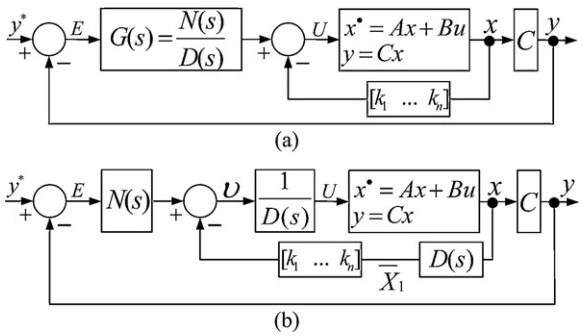

Fig. 17. Block diagram of general LQT-based control system.

Table 3
Steady-state characteristics of the UPS inverter system.

Load	Regulation design		Tracking design	
	Linear	Non-linear	Linear	Non-linear
$V_{o(\mathrm{THD})}$	0.05%	2.32%	.0%	2.1%
Error_{Vo}		≈0%		

Note that in cost function of (30), the corresponding Q_1 matrix can be written as

$$Q_1 = \begin{bmatrix} 0 & \cdots & 0 & 0 \\ \vdots & \ddots & \vdots & \vdots \\ 0 & \cdots & 0 & 0 \\ 0 & \cdots & 0 & h \end{bmatrix}_{(n+r)\times(n+r)} \tag{39}$$

This concludes that the tracking problem can be addressed by a regulation problem on this system via the Q_1 matrix.

6. Results and discussion

The presented techniques for optimal tuning of controllers are based on linear model of the system and the presented simulations in Sections 4 and 5 do not consider the nonlinearities. To verify performances of the proposed controllers in a more realistic scenario, the UPS and DG systems are simulated within the EMTDC/PSCAD environment. The controllers gains are tuned using the proposed algorithms. Results are summarized as follows.

6.1. UPS system

A half-bridge UPS inverter with an output *LC*-filter is simulated with power and control stages parameters stated in Sections 4.1 and 5.1 for regulation and tracking problems. The UPS inverter supplies both linear and nonlinear loads which are compliant with IEC 62040-3 standard for class-I UPS. The steady state characteristics of the system are summarized in Table 3. The output voltage has a low THD with zero steady state error in the RMS value. In addition, Fig. 18 shows the reference voltage, output voltage and current signals for both linear and non-linear loads when the first LQR-based technique is used to tune the controller gains. Fig. 19 presents similar results when the proposed tracking-based controller is used. Both figures confirm the desired transient response of the closed-loop system.

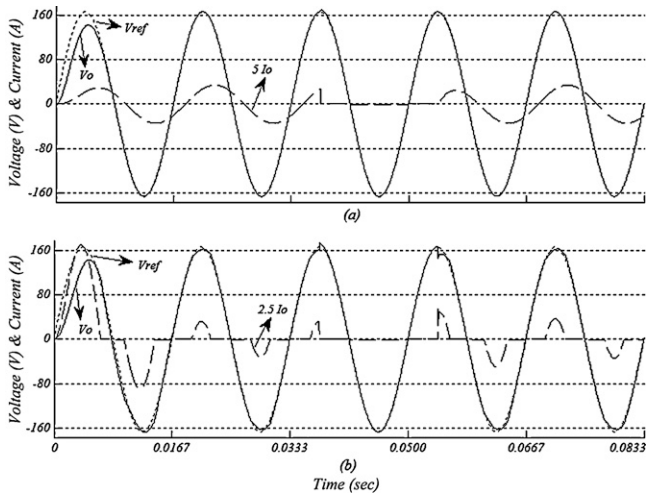

Fig. 18. PSCAD simulation results of UPS inverter with proposed LQR controller design which supplies (a) a linear load (b) a non-linear load.

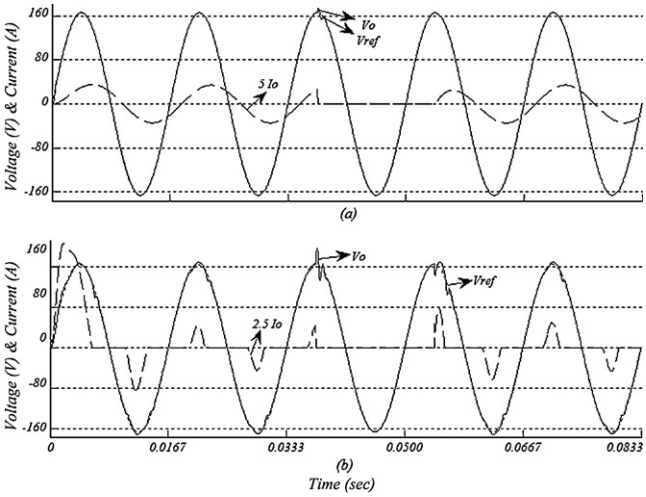

Fig. 19. PSCAD simulation results of UPS inverter with proposed tracking controller design which supplies (a) a linear load (b) a non-linear load.

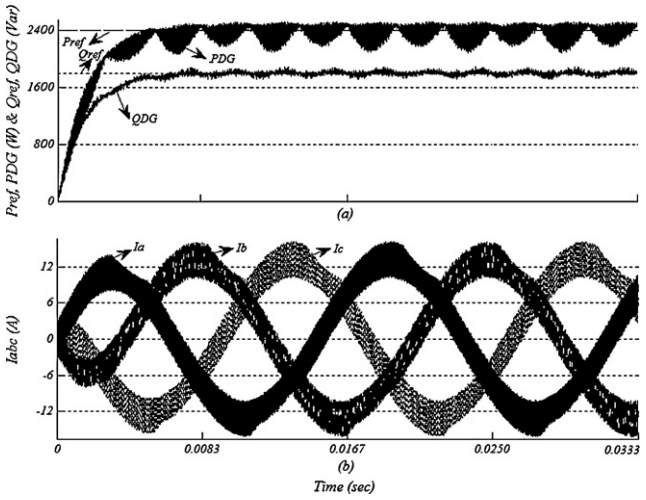

Fig. 20. PSCAD simulation results of DG unit with proposed LQR-based controller (a) output power (b) output current.

6.2. DG unit

A three-phase three-leg inverter-based DG unit is connected to an infinite bus by an inductor. This system is simulated in PSCAD with the power and control stages parameters stated in Sections 4.2 and 5.2. Fig. 20 shows the transient response of the closed-loop system to a real-power command when the LQR-based controller is in operation. Fig. 21 shows similar results when the tracking-based controller is used. The steady-state characteristics of both systems are also shown in Table 4. Both methods offer desirable transient and steady-state performance, yet the tracking-based controller exhibits some improved smoothness of the signals which results in considerable reduction of the current THD. This can be explained using the fact that the tracking controller aims at minimizing the tracking error directly while the LQR controller does this in an indirect manner without particular emphasis on the tracking error.

Table 4
Simulation results of the DG unit.

	Regulation design	Tracking design
$I_{abc(RMS)}$	8.53 A	8.43 A
$I_{abc(THD)}$	2.28%	0.54%
Error(P_{DG}, Q_{DG})	≈0%	

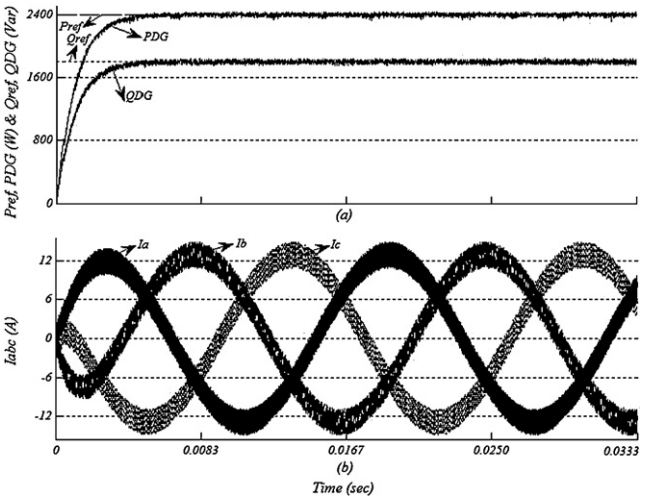

Fig. 21. PSCAD simulation results of proposed tracking-based DG unit controller (a) output power (b) output current.

7. Conclusion

The LQR technique is a well-known method used for optimal tuning of controllers. This method, however, can only address a state-feedback controller used in the context of a regulation problem. In practice, it is often necessary to use an output-feedback controller instead and a tracking problem is the objective to be attained. This paper presents two methods of adjusting LQR parameters to achieve desired tracking characteristics as well as regulation. First, the regulation problem is finally addressed using the LQR method. Next, a new method, which is named tracking-based, is also proposed and generalized to systems with more than two states. The method is capable of tuning controller parameters to directly achieve improved output tracking. The controllers used in this paper are conventional output-feedback controllers such as PI, PID and PR. A contribution of the paper is to represent the closed-loop equations of the output-feedback control in a state-feedback form. The Q matrix is then determined to properly place the closed-loop poles in order to achieve desired transient response. The proposed techniques of this paper are effective, simple to implement, algorithmic and the design procedure is transparent. It avoids complicated classical Bode diagrams and/or root-locus design techniques, without any stability concerns, while still offering an optimal solution with adequate gain and phase margins while ensuring system stability during whole design process. These tuning methods can also be employed by linear state-space realization of any power converters. Both methods are examined on a UPS and a DG control systems. The controllers are designed and the overall systems are simulated in PSCAD. Desired performances of the proposed controllers are observed from the simulations.

Acknowledgement

The authors would like to thank Dr. M. Karimi Ghartemani. of Sharif University of Technology, Tehran, Iran, for his valuable discussion. Additionally, we would like to thank the Florida State University's Institute for Energy Sustainability and Economic Studies for funding the effort.

References

[1] B.A. Francis, W.M. Wonham, The internal model principle of control theory, Automatica 12 (5) (1976) 457–465.
[2] B. Strah, O. Kuljaca, Z. Vukic, Speed active power control of hydro turbine unit, IEEE Trans. Energy Conv. 20 (2) (2005) 424–434.
[3] Y.W. Li, D.M. Vilathgamuwa, P.C. Loh, A grid-interfacing power quality compensator for three-phase three-wire microgrid applications, IEEE Trans. Power Electron. 21 (4) (2006) 1021–1031.
[4] A. Hasanzadeh, O.C. Onar, H. Mokhtari, A. Khaligh, A proportional-resonant controller based wireless control strategy with reduced number of sensors for parallel operated UPSs, IEEE Trans. Power Deliv. 25 (1) (2010) 468–478.
[5] M. Liserre, R. Teodorescu, F. Blaabjerg, Multiple harmonics control for three-phase grid converter systems with the use of PI-RES current controller in a rotating frame, IEEE Trans. Power Electron. 21 (3) (2006) 836–841.
[6] Y. Liao, H. Li, J. Yao, K. Zhuang, Operation and control of a grid-connected DFIG-based wind turbine with series grid-side converter during network unbalance, Electr. Power Syst. Res. 81 (2011) 228–236.
[7] L. Corradini, P. Mattavelli, W. Stefanutti, S. Saggini, Simplified model reference-based autotuning for digitally controlled SMPS, IEEE Trans. power Electron. 23 (4) (2008) 1956–1963.
[8] Y.W. Li, Control resonance damping of voltage source and current source converters with LC filters, IEEE Trans. Ind. Electron. 56 (5) (2009) 1511–1521.
[9] A. Dell'Aquila, M. Liserre, V.G. Monopoli, P. Rotondo, Overview of PI-based solutions for the control of DC buses of a single-phase H-bridge multilevel active rectifier, IEEE Trans. Ind. Appl. 44 (3) (2008) 857–866.
[10] S. Hameed, B. Das, V. Pant, A self-tuning fuzzy PI controller for TCSC to improve power system stability, Electr. Power Syst. Res. 78 (2008) 1726–1735.
[11] V. Mukherjee, S.P. Ghoshal, Intelligent Particle Swarm optimized fuzzy PID controller for AVR system, Electr. Power Syst. Res. 77 (2007) 1689–1698.
[12] T. Amraee, A.M. Ranjbar, R. Feuillet, Adaptive under-voltage load shedding Scheme using model predictive control, Electr. Power Syst. Res. 81 (2011) 1507–1513.
[13] Y. Zhang, L.S. Shieh, A.C. Dunn, PID controller design for disturbed multivariable systems, IEE Proc. Control. Theory Appl. 151 (5) (2004) 567–576.
[14] H. Kmurcugil, O. Kukrer, A. Doganalp, Optimal control for single-phase UPS inverters based on linear quadratic regulator approach, in: Proc. of the Int. Symp. on Power Electron., Electr. Drives, Autom. and Motion, SPEEDAM, 2006, S8-24-29.
[15] Y. Srinivasa Rao, M.C. Chandorkar, Real-time electrical load emulator using optimal feedback control technique, IEEE Trans. Ind. Electron. 57 (4) (2010) 1217–1225.
[16] X. Sun, L-K. Wong, Y-S. Lee, D. Xu, Design analysis of an optimal controller for parallel multi-inverter systems, IEEE Trans. Circ. Syst. II 52 (1) (2006) 56–61.
[17] E. Wu, P.W. Lehn, Digital current control of a voltage source converter with active damping of LCL resonance, IEEE Trans. Ind. Electron. 21 (5) (2006) 1364–1373.
[18] F. Wu, X.P. Zhang, P. Ju, M.J.H. Sterling, Decentralized nonlinear control of wind turbine with doubly fed induction generator, IEEE Trans. Power Syst. 23 (2) (2008) 613–621.
[19] D.E. Kim, D.C. Lee, Feedback linearization control of three-phase UPS inverter systems, IEEE Trans. Ind. Electron. 57 (3) (2010) 963–968.
[20] B.D.O. Anderson, J.B. Moore, Optimal Control Linear Quadratic Methods, Prentice-Hall, Int., 1989.
[21] F. Lin, An optimal control approach to robust control design, Int. J. Control 73 (3) (2000) 177–186.
[22] F. Lin, Robust Control Design: An Optimal Control Approach, John Wiley & Sons Ltd., West Sussex, England, 2007.
[23] H. Tan, S. Shu, F. Lin, An optimal control approach to robust tracking of linear systems, Int. J. Control 82 (3) (2009) 525–540.
[24] M.G. Safonov, M. Athans, Gain and phase margin for multi-loop LQG regulators, IEEE Trans. Autom. Control. 22 (2) (1977) 173–179.
[25] R.E. Kalman, Contributions to the theory of optimal control, Bol. Sot. Matem Mex. 10 (1960) 2–119.
[26] M.J. Ryan, W.E. Brumsickle, R.D. Lorenz, Control topology options for single-phase UPS inverters, IEEE Trans. Ind. Appl. 33 (2) (1997) 493–501.